Adsorption (2007) 13: 587–601
DOI 10.1007/s10450-007-9029-1

Modeling equilibrium and kinetics of metal uptake by algal biomass in continuous stirred and packed bed adsorbers

Vítor J.P. Vilar · Cidália M.S. Botelho · Rui A.R. Boaventura

Received: 3 April 2007 / Revised: 16 July 2007 / Accepted: 23 July 2007 / Published online: 21 September 2007

Abstract Physical and chemical characterization of algae *Gelidium* particles shows a gel structure, with two major binding groups, carboxylic and hydroxyl groups, with an affinity constant distribution for protons, well described by a Quasi-Gaussian distribution suggested by Sips. A continuous model, considering a heterogeneous distribution of the carboxylic groups, determined by potentiometric titration experiments, was able to predict equilibrium data at different pH. The metal uptake capacity decreases with the solution pH, suggesting that competition exists between hydrogen ions, present in high concentrations for low pH values, and metal ions. For high ionic strengths, adsorption sites will be surrounded by counter ions and partially lose their charge, which weakens the contribution of the electrostatic binding and decreases the overall adsorption. A small influence of the temperature in the adsorption process was observed. Batch kinetic experiments were also performed, at different pH values, and results were well fitted by a mass transfer model, considering the intraparticle diffusion resistance given by the linear driving force model (LDF). Continuous stirred adsorber (CSTA) and packed bed column configurations were also tested for metal adsorption. The biosorbent regeneration was achieved by contacting it with strong acid (0.1 M HNO_3). A mass transfer model was applied with success to describe the biosorption/desorption process in CSTA and packed bed column, considering the equilibrium given by the Langmuir equation/mass action law and film and intraparticle diffusion resistances.

Keywords Biosorption · Desorption · Metals · Modeling · Algae *Gelidium sesquipedale*

Abbreviations

a_p	Specific area for thin plates particles
C_b	Metal concentration in the bulk (mg or mmol metal/l fluid)
C_{b_0}	Initial metal concentration in the bulk (mg or mmol metal/l fluid)
C_E	Feed concentration (mg or mmol metal/l fluid)
C_f	Metal concentration in the film (mg or mmol metal/l fluid)
C_{final}	Metal concentration in the solution at the end of the saturation or elution process (mg or mmol metal/l fluid)
C_{CI}	Initial metal concentration in the solution (elution process) (mmol metal/l fluid)
C_H	Equilibrium concentration of proton in the fluid phase (mmol proton/l fluid)
C_M	Equilibrium concentration of metal in the fluid phase (mmol metal/l fluid)
C_T	Total (metal + acid) liquid concentration (mmol/l fluid)
C_{T_0}	Initial total (metal + acid) liquid concentration (mmol/l fluid)
C_{T_E}	Total feed (acid) liquid concentration (mmol/l fluid)
D_{ax}	Axial dispersion coefficient (cm^2/s)
D_h	Homogeneous diffusion coefficient (cm^2/s)
IS	Ionic strength (M)

V.J.P. Vilar · C.M.S. Botelho · R.A.R. Boaventura (✉)
LSRE Laboratory of Separation and Reaction Engineering, Department of Chemical Engineering, Faculty of Engineering, University of Porto, Rua Dr. Roberto Frias, 4200-465 Porto, Portugal
e-mail: bventura@fe.up.pt

V.J.P. Vilar
e-mail: vilar@fe.up.pt

C.M.S. Botelho
e-mail: cbotelho@fe.up.pt

k_f	Film mass transfer coefficient (cm/s)
k_p	Mass transfer coefficient for intraparticle diffusion (cm/s)
K_H	Equilibrium proton constant (l fluid/mmol H)
K_M	Equilibrium metal constant (l fluid/mmol M)
K'_H	Average value of the affinity constant distribution for the proton (l fluid/mmol H)
K'_M	Average value of the affinity constant distribution for the metal (l fluid/mmol M)
K_L	Equilibrium constant of Langmuir (l fluid/mg M)
K_H^M	Selectivity coefficient between ion M in the particle and ion H in solution
L	Bed length (cm)
n	Empirical dimensionless parameter
n_M and n_H	Constants that reflect the overall non-ideality of metal and proton
N_d	Number of mass transfer units by intraparticle diffusion
N_f	Number of mass transfer units by film diffusion
p	Represents the intrinsic heterogeneity of the biosorbent
Pe	Axial Peclet number based on the bed length
Pe_p	Axial Peclet number based on the particle diameter (spherical) or width (thin plate)
pH_{SE}	pH of feed solution
$\langle q \rangle$	Average metal concentration in the solid phase (mg or mmol metal/g biomass)
q_E	Solid phase concentration in equilibrium with C_E (mg or mmol metal/g biomass)
q_H	Equilibrium concentration of proton in the biomass (mmol metal/g biomass)
q_L e q_{LF}	Maximum amount of metal per g of adsorbent (mg/l)
q_M	Equilibrium concentration of metal in the biomass (mg or mmol metal/g biomass)
q_{M_0}	Metal concentration in the solid phase in equilibrium with C_{b_o} (mg or mmol metal/g biomass)
q^*	Solid phase concentration in equilibrium with C_f (mg or mmol metal/g biomass)
q_t	Concentration of ion species in the sorbent at time t (mg metal g biosorbent^{-1})
$Q_{\max}$	Concentration of carboxylic groups or maximum capacity of biomass (mmol/g biomass)
r	The dimensionless axial coordinate inside the particle
R	Half of thickness of the thin plate (cm)
Sh	Sherwood number
t	Time (s)
t_b	Breakthrough time (s)
t_{st}	Stoichiometric time (s)
T	Temperature (°C)
u_i	Interstitial fluid velocity (cm/s)
V	Metal solution volume (l)
V_r	Volume of the adsorber (CSTA) (cm^3)
x	Axial position normalized by the bed length
$\langle y \rangle$	Dimensionless average concentration in the solid phase
y'_b or y_b	Dimensionless concentration in the fluid phase
y'_f	Dimensionless concentration in the fluid phase at the film
y_T	Dimensionless total concentration in the fluid phase
y^* or y_M	Dimensionless concentration in the solid phase at the particle surface
z	The distance to the symmetry plane (cm)
z'	Bed axial position (cm)
W	Mass of biosorbent (g)
ε	Porosity of the bed
τ	Space time (s)
τ_d	Time constant for intraparticle diffusion
τ_f	Time constant for film diffusion
θ	Dimensionless time
ρ_{ap}	Apparent density of particles (g solid/cm^3 particle)
ξ	The batch capacity factor
ξ'	Adsorber capacity factor for saturation
ξ''	Adsorber capacity factor for desorption

1 Introduction

Heavy metal pollution is a threat to human health, animals, plants, and the planet itself, and is mainly caused by industrialization and its consequences. The search for new technologies involving the removal of toxic metals from wastewaters has directed attention to biosorption, based on metal binding capacities of various biological materials. The major advantages of biosorption over conventional treatment methods include (Kratochvil and Volesky 1998): low cost; high efficiency; minimization of chemical and or biological sludge, no additional nutrient requirements, regeneration of biosorbent and possibility of metal recovery.

Over the last two decades, research on different types of biosorbents has been performed in order to develop a biosorption technology, capable of open new opportunities in the environment market. Although different kinds of biosorbents have been tested to remove several metals (Bailey et al. 1999; Babel and Kurniawan 2003) only few have been commercialized. The algal biosorbent Alga SORB^{TM} was developed by Bio-recovery Systems Inc., using the freshwater algae *Chrorella vulgaris* to treat wastewater contaminated with metal ions (Volesky 1990). B.V. Sorbex has

developed different biosorbents for specific metal recovery using different types of biomass, including the algae *Sargassum natans*, *Ascophyllum nodosum*, *Halimeda opuntia*, *Palmyra pamada*, *Chondrus crispus* and *Chlorella vulgaris* (Wase and Forster 1997). Other commercial biosorbents have been produced, such as AMT-BIOCLAIM, using the *Bacillus* biomass (Volesky 1990), Bio-Fix, using a granular biosorbent consisting of a variety of biomasses including algae immobilized in porous polypropylene beads (Wase and Forster 1997), MetaGeneR and RAHCO Bio-Beads (Atkinson et al. 1998; Gavrilescu 2004). In all these systems, as it is the case for most sorption processes in general, the biosorbent is used as a packed bed contacting a downflow stream. This is the most effective configuration (Volesky 2001).

This paper presents the conception and optimization of the biosorption process according to the following steps: (1) biosorbent characterization; (2) determination of equilibrium (biosorption/desorption) relationships; (3) determination of the biosorption/desorption kinetics; (4) determination of the breakthrough time in a continuous stirred tank ("Carberry" type) and a packed bed column, using as biosorbent, the algae *Gelidium sesquipedale*, a red algae harvested in the coast of Portugal.

2 Materials and methods

2.1 Preparation of the biosorbent

Algae *Gelidium* sesquipedale harvested in the coasts of Algarve and São Martinho do Porto, Portugal, was used in this study. Algal samples were washed several times with distilled water, dried in an oven at 60 °C and sieved, obtaining thin plates particles of dead algae. The characteristics and preparation of the material was presented in previous works (Vilar et al. 2005b, 2006a).

2.2 Preparation of metal solutions

Copper(II), lead(II) and cadmium (II) solutions were prepared by dissolving a weighed quantity of, respectively, $CuCl_2 \cdot 2H_2O$ (Riedel-de-Haën, purity >99%), anhydrous $PbCl_2$ (Merck-Schuchardt, purity >98%) and $CdCl_2$ (Sigma-Aldrich >99%) in distilled water. The ionic strength was adjusted by using 1 M KNO_3 (Merck >99%). The pH was controlled by adding 0.01 M HCl or 0.01 M NaOH solutions.

2.3 Biosorbent characterization

Data concerning the specific surface area (A_{sp}) (methylene blue adsorption, N_2 adsorption at 77 K and mercury intrusion methods), equivalent length, width and thickness (SEM and image analysis), apparent density (ρ_{ap}), pore volume (V_p) and porosity (ε_P) (by mercury intrusion in a Micromerities Poresizer 9320), real density (ρ_{re}) (helium picnometry-ACCUPYC 1330), total organic carbon (TOC-Shimadzu Izasa 5000 A), volatile matter, metal ions concentration (GBC 932 Plus Atomic Absorption Spectrometer), type and amount of binding groups at the algae surface (FTIR analysis-FTIR Bomen, Arid-Zone^{TM} 1540 and potentiometric titration, respectively) are presented in Table 1.

2.4 Sorption studies

Batch biosorption dynamic experiments were carried out in a 1-liter capacity glass vessel, equipped with a cooling jacket (Grant type VFP) to ensure a constant temperature of 20 °C during the experiment. The pH was also monitored and controlled (WTW 538 pH/temperature meter). The equilibrium experiments were performed in duplicate, using 100 ml Erlenmeyer flasks, at constant pH, ionic strength and temperature. Details about the experimental procedure were presented elsewhere (Vilar et al. 2005a).

Table 1 Physical and chemical characteristics of algae *Gelidium sesquipedale*

Physical characteristics		Chemical characteristics			
ρ_{ap} (g cm^{-3})	1.34[a]	TOC (mg l^{-1})	46.7[b]	Pb, Cd, Zn, Cu, Cr, Ni (mg g^{-1})	$<7 \times 10^{-3}$[b]
ρ_{re} (g cm^{-3})	1.46[a]	Volatile matter (%)	94.4[b]	Al (mg g^{-1})	0.14[b]
ε_P	0.08[a]	$Q_{max,1}$ (mmol g^{-1})	0.36 ± 0.01[b]	Fe (mg g^{-1})	0.14 [b]
V_p (total) (cm^3 g^{-1})	0.126[a]	$Q_{max,2}$ (mmol g^{-1})	0.15 ± 0.01[b]	Mn (mg g^{-1})	3.3×10^{-2}[b]
A_{sp} (m^2 g^{-1})	71 ± 2[a]	$pK'_{1,H}$	5.0 ± 0.1[b]	K (mg g^{-1})	3.6 [b]
Length (mm)	2.5 ± 0.7[a]	$pK'_{2,H}$	9.2 ± 0.1[b]	Na (mg g^{-1})	1.9 [b]
Width (mm)	0.6 ± 0.1[a]	$m_{H,1}$	0.4 ± 0.1[b]	Ca (mg g^{-1})	5.3 [b]
Thickness (mm)	0.1[a]	$m_{H,2}$	0.6 ± 0.1[b]	Mg (mg g^{-1})	4.6 [b]

[a]Vilar et al. (2006b)

[b]Vilar (2006)

2.5 Adsorber continuous experiments

CSTA experiments were conducted in a "Carberry" well mixed adsorber (mechanical stirrer Heidolph) with hampers packed with algae *Gelidium* particles. The useful adsorber volume is 540 cm^3, which gives a residence time of 15.2 ± 0.4 min. An acrylic jacket surrounding the CSTA adsorber body allows the operation at constant temperature. A known quantity of algae *Gelidium* ($\approx$10 g) was placed into the hampers. The metal solution (25.5 $mg\,l^{-1}$) was pumped (peristaltic pump Ismatec Ecoline VC-380) through the CSTA at 35.5 $ml\,min^{-1}$. Effluent samples were collected regularly and analyzed by Atomic Absorption Spectrometry (AAS). The pH of the effluent was continuously monitored. At the end of the sorption process, the metal loaded biomass was regenerated using 0.1 M HNO_3.

2.6 Column experiments

Column experiments were conducted in a glass column (Sigma C 5794) with 2.5 cm inner diameter and 15 cm length (L) packed with algae *Gelidium* particles. Temperature was maintained constant by circulating water through an acrylic jacket surrounding the column body. Adjustable plungers, with 20 μm selective filters, were attached to the top and bottom of the column. Around 10 g of algae was placed into the column. Metal solution (50 $mg\,l^{-1}$) was pumped through the column at 4 $ml\,min^{-1}$ (peristaltic pump Gilson Minipuls 2). Samples from the column effluent were collected regularly by a programmable fraction collector (Gilson FC 203B Fraction Collector) and analyzed by AAS. The effluent pH was permanently recorded. After column saturation, a regeneration process using 0.1 M HNO_3 at 8 $ml\,min^{-1}$ was performed. The sample collection and analytical procedure were the same as for the adsorption step. The biomass dried weight was obtained by drying the particles at 50 °C during two days. The column was washed with nitric acid (20%) and distilled water to remove all the contaminants.

2.7 Analytical procedure

Metal concentration was determined by AAS (GBC 932 Plus Atomic Absorption Spectrometer). The working current/wavelength was adjusted to 3.0 mA/324.7 nm-Cu; 3.0 mA/228.8 nm-Cd; 5.0 mA/217.0 nm-Pb, giving a detection limit of 0.2 ppm (Cu and Cd) and 0.4 ppm (Pb). The instrument response was periodically checked with Cu(II), Cd(II) and Pb(II) standard solutions.

3 Results and discussion

3.1 Biosorbents characterization

The algae *Gelidium sesquipedale* particles are like thin plates, with a length and width that greatly exceed the thickness. The values where obtained by image analysis and SEM. The average value and standard deviation of the size distribution is presented in Table 1. This results were also presented in a previous paper, including the distribution of the three dimensions (Vilar et al. 2006b).

Algae *Gelidium* has a low porosity, suggesting that the sample can't tolerate a high pressure in mercury intrusion without collapsing or compressing. Between 8 and 0.1 μm the intrusion curve presents a linear increase with pressure (data not shown), which is often interpreted as the collapse of the porous structure (Vilar et al. 2006b).

The surface of the biosorbents was determined by the methylene blue adsorption and mercury intrusion methods and nitrogen adsorption-desorption isotherms at 77 K, using the BET method. In aqueous solution MB molecule is cationic, so, adsorption can be due to the electrostatic interaction between the negative charged groups present in the materials and the positive charge of the MB molecule, as occurs in the metal biosorption. Mercury intrusion method gives lower values, related to the collapse of the non rigid porous structure. The low values of specific surface area obtained by the N_2 adsorption method are due to the fact that all pores are closed in the vacuum-dried state, which promotes the formation of interchain hydrogen linkages or cellulose-cellulose linkages, which are too strong to be replaced by N_2 molecules (Vilar et al. 2006b).

The algae *Gelidium sesquipedale* used in this work has been investigated by different authors (Vignon et al. 1994a, 1994b; Davis et al. 2003), due to economic reasons, as it is the main commercial source for agar industry. The composition of cell wall is: agarose (43%), starch/amylase and biological precursors (7%), proteins (24–28%) and cellulose (8–10%), which represents at least 82% of the dried algae (Table 2). In the structure of these constituents we can find mainly carboxyl (D-glucuronic and pyruvic acids) and hydroxyl groups (Cellulose, Agar, Floridean starch), as demonstrated by FTIR analysis and potentiometric titrations (Vilar 2006). Considering the surface of the biosorbents as polifunctional, each active site, of one certain functional group, will react with protons with a different affinity and the total fraction of protonated sites, $\theta_{T,H}$, can be given by a Langmuir–Freundlich isotherm, assuming a Quasi-Gaussian distribution of the affinity constant suggested by Sips (Sips 1948):

$$\theta_{T,H} = \frac{(K'_H C_H)^{m_H}}{1 + (K'_H C_H)^{m_H}} \quad (1)$$

Table 2 Main constituents of algae *Gelidium sesquipedale*

Constituents		Monomer	Groups	Function	% (dry weight)
Cellulose	Glucose	Glucose	CH_2OH; OH	Cell wal	(8–10)[b]
Agar	Agarose	Glucose	CH_2OH, OH		43[b]; (55–60)[a]
	Agaropectin	D-glucuronic acid	COOH, OH		7[b]; (3.5–9.7)[a]
		Pyruvic acid	COOH, OH		
	Galactans	Ester sulfonate	OSO_3^-		(1.0–1.6)[b]
Floridean starch		Glucose	CH_2OH; OH	Storage product	Storage product

[a]Volesky (2003)

[b]Vignon et al. (1994a), Mouradi-Givernaud et al. (1999)

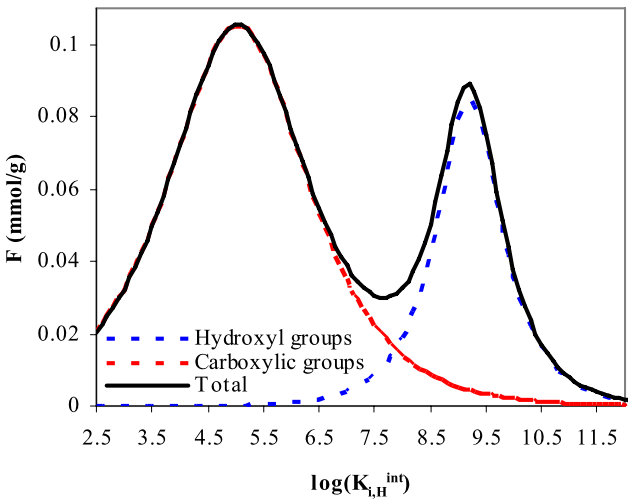

Fig. 1 Affinity distribution function for protons $F = \sum_i f_i \times (\log K_{i,H}^{\text{int}}) Q_{\max,i}$ for algae *Gelidium*

where K'_H is the average value of the affinity distribution for the proton, which determines the position of the affinity distribution on the $\log K_{i,H}^{\text{int}}$ axis, C_H is the concentration of the proton in the solution, and m_H $(0 < m_H < 1)$ is the width of their peak in the Sips distribution (the extreme values 0 and 1 represent a null or infinite width, respectively). The charge of a biosorbent depends on the degree of protonation. If the affinity distribution exhibits more than one peak, then the charge of an acidic surface, Q_H, is expressed as the weighted summation of the charge contributions of the different site types:

$$Q_H = \sum_j Q_{\max,j}(1 - (\theta_{T,H})_j) \tag{2}$$

where $Q_{\max,j}$ is the overall charge of the binding group j.

Figure 1 represents the continuous affinity distribution of the carboxylic and hydroxyl binding groups given by a Quasi-Gaussian distribution suggested by Sips for algae *Gelidium sesquipedale*, whose parameters are presented in Table 1. The distribution of affinity constants shows two peaks, one for carboxylic groups and the other for hydroxyl groups. The heterogeneity is given by the width of the distribution, m_H (low m_H values correspond to a wider distribution and to a higher heterogeneity of the groups). Constant affinity distribution shows higher heterogeneity on the binding to carboxyl groups.

3.2 Equilibrium modeling

Different kinds of equilibrium models have been used to describe biosorption equilibrium data, as Langmuir (1918), Freundlich (1907), Langmuir-Freundlich combination (Sips 1948), Redlich-Petterson (Redlich and Peterson 1959), Brunauer Emmett Teller (Brunauer et al. 1938), Radke and Prausnitz (1972), and others. As these equilibrium models, in their simple form, do not consider the heterogeneity of the binding sites, the pH influence on the biosorption process and hardly reflect the sorption mechanism, discrete and continuous affinity distribution equilibrium models, considering an complexation mechanism and non ideal competitive adsorption (NICA) have been used successfully to describe biosorption of Cu(II), Pb(II) and Cd(II) by algae *Gelidium* (Vilar 2006; Vilar et al. 2007c). Assuming one kind of active sites (carboxylic groups) in the cell wall, responsible for metal biosorption at pH < 7, and competition between metal ions and protons, a discrete equilibrium model based on apparent equilibrium binding constants, K_H and K_M for H^+ and M^{2+}, respectively, the total metal uptake can be calculated as:

$$q_M = \frac{Q_{\max} K_M C_M}{1 + K_H C_H + K_M C_M}. \tag{3}$$

This equation can be converted to a Langmuir-type equation dividing by $(1 + K_H C_H)$:

$$q_M = \frac{Q_{\max} K'_L C_M}{1 + K'_L C_M}, \quad K'_L = \frac{K_M}{1 + K_H C_H}. \tag{4}$$

For an adsorbent with heterogeneous active sites, assuming competition between metal ions and protons, and that metal

ions biosorption occurs only on carboxylic groups (pH < 7), a Non Ideal Competitive Adsorption model (NICA) can be defined as (Kinniburgh et al. 1999):

$$q_M = Q_{\max}\frac{n_M}{n_H} \times \frac{(K'_M C_M)^{n_M}\{(K'_H C_H)^{n_H} + (K'_M C_M)^{n_M}\}^{p-1}}{1 + \{(K'_H C_H)^{n_H} + (K'_M C_M)^{n_M}\}^{p}} \quad (5)$$

where n_M and n_H reflect the overall non-ideality which can be due to lateral interactions and/or stoichiometry effects. The effect of the groups intrinsic heterogeneity (p) can be isolated from the non-ideal behavior of metal and proton ($n_{M,}$ and n_H), since $m_i = n_i \times p$. Applying the NICA model to the equilibrium Cu(II) data, we obtain the three dimensional surface represented in Fig. 2a, which describes well the experimental results. Figure 2b represents the affinity distribution function for the binding of Cu(II), Pb(II) and Cd(II) to algae *Gelidium* carboxylic groups, obtained by the Sips distribution using the NICA model parameters (Vilar 2006; Vilar et al. 2007c). Figure 2b shows that the Cu(II) binds to ligands more homogeneous, which means, with narrow distribution of the affinity constant, while Pb(II) and Cd(II) present a wider distribution of the affinity binding constant.

Metal ions act as Lewis acids by accepting electron pairs from ligands. Class A metal ions, also called hard or nonpolarizable, preferentially form complexes with similar nonpolarizable ligands, particularly oxygen donors, and the binding is mainly ionic. Class B or soft metal ions preferentially bind to polarizable soft ligands (S), to give a rather more covalent bonding (Pearson 1963). Lead, copper and cadmium ions are considered as borderline metals. The affinity increases in the following order Cd(II) < Cu(II) < Pb(II) for algae *Gelidium* (Vilar 2006; Vilar et al. 2007c). The covalent index (product of the electronegativity square by the sum ionic radius + 0.85, which is an appropriate constant assumed to reflect the radius of O and N donor atoms) also increases in the order: Cd(II) (5.20) < Cu(II) (6.32) < Pb(II) (6.61) (Nieboer and McBryde 1973). In general, the greater the covalent index of a metal ion, the greater its Class B character, and consequently its potential to form covalent bonds with biological ligands.

3.2.1 *Influence of pH*

The influence of the metal solution pH in the biosorption process is of great importance. It is expected that pH influences both metal binding sites on the cell surface and metal chemistry in water. For pH 3 a significant inhibition of biosorption is observed (Fig. 3a), as cell wall ligands are closely associated with hydronium ions, which restrict the approach of metal cations as a result of repulsive forces. On

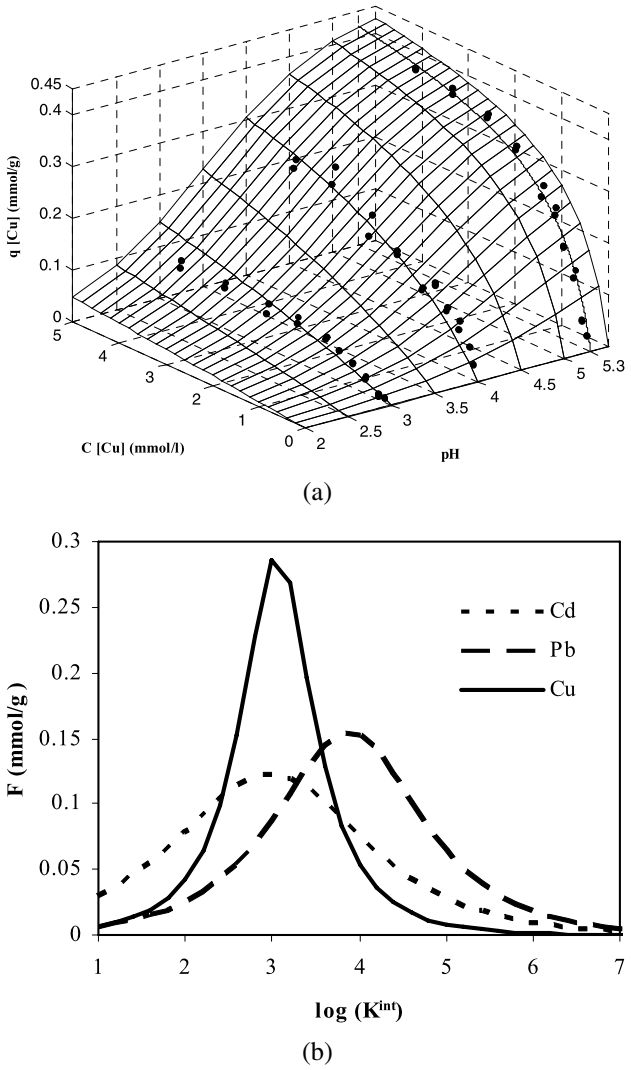

Fig. 2 **a** Copper sorption isotherm surface for algae *Gelidium*: experimental data and continuous equilibrium model mesh. Solution pH 3, 4 and 5.3, copper concentration 0.0 to 5.0 mmol l^{-1}; **b** Affinity distribution function of Cu(II), Pb(II) and Cd(II) for carboxylic groups

the other hand, proton competes with metal ions for the active sites on biomass surface and so a remarkable inhibition is observed (Vilar et al. 2005a, 2006a, 2007c). As the pH increases, more ligands with higher affinity to the metal ions, carrying negative charges, attract the metal ions, and biosorption onto cell surface increases (Fig. 3b). High pH values lead to precipitation of metal ions, and low pH values, as employed for regeneration of biosorbents, can damage the biomass structure.

3.2.2 *Temperature*

The temperature can influence the biosorption process positively and negatively, which means that the biosorption process can be exothermic or endothermic. The increase of the binding capacity with temperature can be attributed to

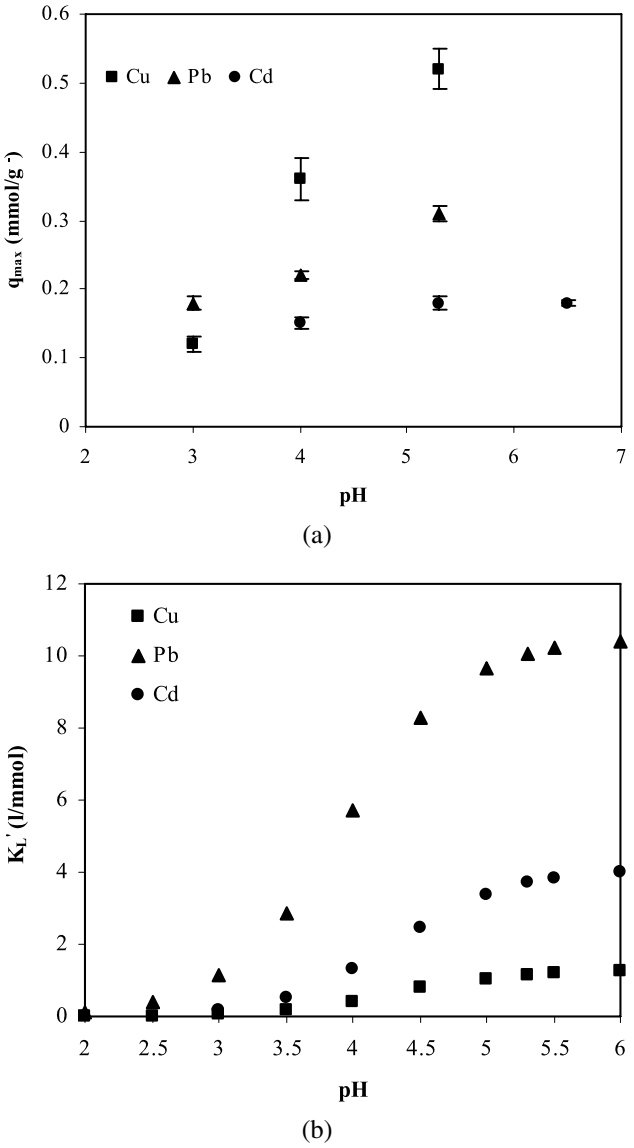

Fig. 3 Effect of the pH on the values of Langmuir q_{max} **(a)** and K_L' **(b)** for algae *Gelidium*

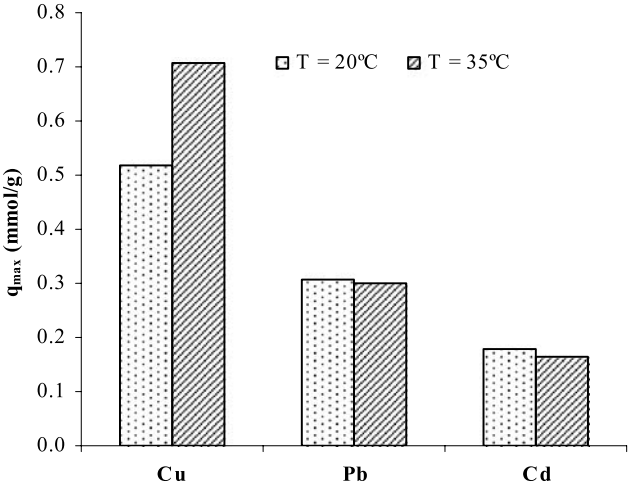

Fig. 4 Effect of temperature on Cu(II), Pb(II) and Cd(II) uptake capacity of algae *Gelidium*

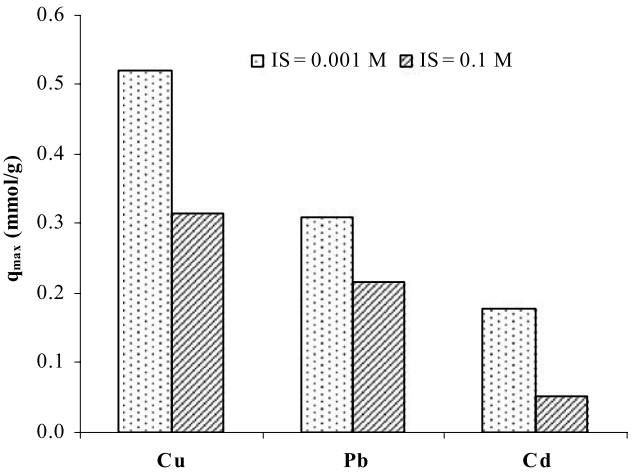

Fig. 5 Effect of ionic strength on Cu(II), Pb(II) and Cd(II) uptake capacity of algae *Gelidium*

the increase in the energy of the system that facilitates the attachment of metal ions to the surface of the active sites or to the fact that some active sites become available (Al-Ashed and Duvnjak 1995). For algae *Gelidium*, it was concluded that Cu(II) biosorption increases ≈36%, when varying the temperature from 20 °C to 35 °C (Fig. 4). For Pb(II) and Cd(II) biosorption, the temperature effect is negligible. The increase in temperature is not economically attractive because it has only a slight effect on the uptake capacity. On the other hand, temperature must be in the range ∼5–60 °C, because higher temperature can destroy the biomass, losing the active sites (Volesky 2003).

3.2.3 *Influence of ionic strength*

The effect of ionic strength on Cu(II), Pb(II) and Cd(II) biosorption was studied by changing the electrolyte (KNO_3) concentration at pH = 5.3. Figure 5 shows that increasing the ionic strength, the biosorption of these metal ions decreases, respectively, 39.4%, 29.7% and 71.2%. For high ionic strengths, the negatively charged adsorption sites are surrounded by counter ions (potassium ions) and partially lose their charge, which weakens the contribution of the electrostatic binding to the overall biosorption capacity.

The influence of IS on the metal uptake follows the order Cd(II) > Cu(II) > Pb(II). When the contribution of the covalent binding to the overall biosorption is higher than the electrostatic binding, the influence of the IS is less noticed. This is in agreement with the covalent index, which is higher for Pb(II).

3.3 Biosorption dynamics in batch and continuous systems

3.3.1 Mass transfer model in a batch system

A mass transfer model capable of describing the dynamic results in a batch system, can give a lot of information to project the biosorption system, decreasing the number of experiments necessary to reach the optimal conditions.

The usual concept of a solid-phase sorbent with physical pores and 'surface area' etc. may not be so close to real structure, appearance and behavior of biosorbent materials. Particularly in conjunction with metal ions as sorbate species, biosorbents may appear as gels, very transparent for the minute ions (Volesky 1990, 2001). Several steps of metal transfer from bulk solution to the binding sites have been reported in the literature: bulk transport of metal ions in the solution phase, diffusion of the metal ions through a hydrodynamic boundary layer around the biosorbent surface, diffusion of the metal ions in the pores of the biosorbent and binding of the metal ions by the active sites on the biomass. Adopting experimental conditions allowing good mixing of solutes and biomass in the system, the kinetic limitations due to the first and second steps are suppressed.

Saturation For a quantitative description of the biosorption batch process dynamics, the following assumptions were made: the effect of the external film diffusion on the biosorption rate is negligible when using adequate stirring; the sorption rate is controlled by homogeneous diffusion inside the particle or by Linear Driving Force (LDF); the biosorption process is isothermal and equilibrium exists between bound and dissolved metal ions, as formulated by the Langmuir isotherm; particles are uni-dimensional thin plates, therefore, the overall sorption rate is controlled by intraparticle diffusion in the direction normal to the surface of the particles. The concentration profiles inside the particle can be predicted either by the homogeneous diffusion model or by the Linear Driving Force model (LDF), but the last one can be analytically solved. During the biosorption process, the diffusion and binding of metal ions into the biomass must be accompanied by the release of protons (or other ions) that diffuses into the bulk solution. The diffusion coefficient for H^+ is higher than that for heavy metal ions present in aqueous solution. Therefore, the assumption that the overall sorption rate is controlled by heavy metal diffusion is reasonable.

Homogeneous diffusion model Mass conservation inside the particles

$$\frac{\partial y(r,t)}{\partial t} = \frac{1}{\tau_d}\frac{\partial^2 y(r,t)}{\partial r^2}, \qquad \tau_d = \frac{R^2}{D_h}. \tag{6}$$

The initial and boundary conditions for (6) are:

$$t=0: \quad y_b(0)=1, \quad 0 \le r < 1, \quad y(r,0)=0, \tag{7}$$

$$r=0: \quad \frac{\partial y(r,t)}{\partial r} = 0 \quad \forall t, \tag{8}$$

$$r=1: \quad \frac{\partial y(r,t)}{\partial t} = -\frac{\xi}{\tau_d} K_L C_{b_0}[1-y(r,t)]^2 \times \left[\frac{\partial y(r,t)}{\partial r}\right]_{r=1} \quad \forall t. \tag{9}$$

Dimensionless variables:

$$y_b(t) = \frac{C_b(t)}{C_{b_0}}, \qquad y(r,t) = \frac{q(z,t)}{Q_{\max}},$$

$$\langle y(r,t)\rangle = \frac{\langle q(z,t)\rangle}{Q_{\max}}, \qquad r = \frac{z}{R},$$

$$y_M(t) = \frac{q_M(t)}{Q_{\max}}, \qquad \xi = \frac{W Q_{\max}}{V C_{b_0}}.$$

A collocation on finite elements method (Madsen and Sincovec 1979) was used to solve the nonlinear parabolic PDE with the initial and boundary conditions for each model equation.

Linear Driving Force model (LDF) If the average metal concentration inside the particle is considered, instead of a concentration profile, the following equations are obtained:

Kinetic law (Glueckauf and Coates 1947):

$$\frac{d\langle y(t)\rangle}{dt} = k_p a_p [y_M - \langle y(t)\rangle], \qquad k_p a_p = \frac{D_h}{\phi R^2} = \frac{3}{\tau_d}, \tag{10}$$

$$\phi = \frac{1}{3}, \qquad a_p = \frac{1}{R}.$$

Mass conservation in the fluid inside the closed vessel:

$$\langle y(t)\rangle = \frac{1}{\xi}(1 - y_b(t)). \tag{11}$$

Initial condition:

$$t=0: \quad y_b(t)=1, \qquad \langle y(t)\rangle = 0. \tag{12}$$

Rearranging (10) and (11) the following expression is obtained that can be solved analytically using the initial conditions of (12):

$$\frac{1}{k_p a_p}\frac{dy_b(t)}{dt} + \left(\frac{\xi K_L C_{b_0}}{1 + K_L C_{b_0} y_b(t)} + 1\right) y_b(t) = 1. \tag{13}$$

Biosorption of Cu(II), Pb(II) and Cd(II) mainly occurs within the first 20 minutes (Vilar et al. 2006a, 2007b, 2007c). Removal of metal ions is faster at the initial stage and gradually decreases with time until saturation. At the initial stage

Table 3 Estimated parameters for the linear driving force (LDF) and homogeneous particle diffusion models

Metal	C_{ini} (mg l^{-1})	pH	LDF model		Homogeneous diffusion model			
			$k_p \times a_p$ (min^{-1})	τ_d (min)	τ_d (min)	D_h (cm^2 s^{-1})	$\overline{D}_h$ (cm^2 s^{-1})	D_m[a]
Cu	95	5.3	0.25	12	12	3.5×10^{-8}	3.2×10^{-8}	7.2×10^{-6}
	94	4.0	0.20	15	13	3.2×10^{-8}		
	94	3.0	0.20	15	15	2.8×10^{-8}		
Pb	104	5.3	0.17	18	17.5	2.4×10^{-8}	3.7×10^{-8}	9.3×10^{-6}
	106	4.0	0.33	9.1	9	4.6×10^{-8}		
	106	3.0	0.30	10	10	4.2×10^{-8}		
Cd	100	6.5	0.33	9.1	9	4.6×10^{-8}	4.7×10^{-8}	7.1×10^{-6}
	95	5.3	0.33	9.1	9	4.6×10^{-8}		
	84	4.0	0.35	8.6	8.6	4.8×10^{-8}		

[a]Dean (1979), Reid et al. (1987)

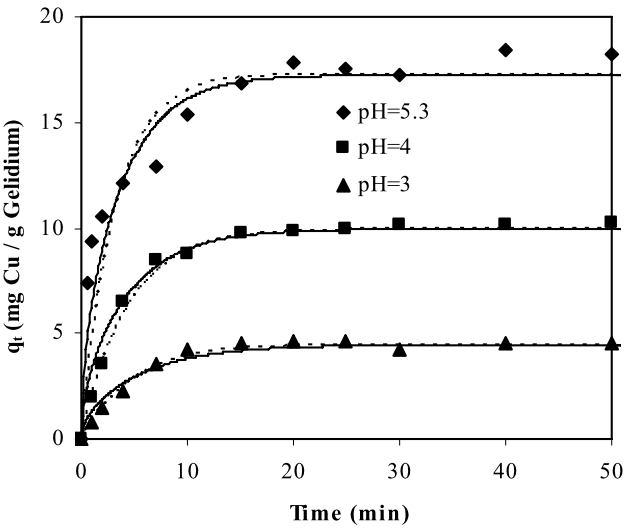

Fig. 6 Evolution of adsorbed Cu(II) concentration on algae *Gelidium* with contact time for different values of pH: experimental data and mass transfer kinetic models (linear driving force model (- - -) and homogeneous diffusion model (——))

the driving force is higher, which permits to overcome all the external mass transfer resistances and the active sites with higher affinity are first occupied. After that, metal concentration in solution decreases, decreasing the driving force, and the remaining active sites with lower affinities are occupied slowly. This behavior is typical for biosorption of metals involving purely weak intermolecular forces between the biomass and the metal in solution. Matheickal and Yu (1999) studied the biosorption of Cu(II) from aqueous solutions by pre-treated biomass of Australian marine algae in batch conditions, concluding that 90% of the adsorption was completed in about 30 min, followed by a 1 h-period of slower uptake rate.

Both mass transfer models fit well the biosorption kinetics for Cu(II) (Fig. 6), Pb(II) and Cd(II) (Vilar et al. 2006a, 2007b, 2007c). The models parameters are presented in Table 3. The obtained average diffusion coefficients are two orders of magnitude below the metal diffusion coefficient in water at 20 °C, due to the resistance to diffusion through the biosorbent particles.

The metal concentration inside the particle follows approximately a parabolic profile for low values of (t/τ_p) and a linear profile near the equilibrium. The average metal concentration ($\langle y \rangle$) inside the particle is initially very different from the metal concentration (y), but as (t/τ_p) increases both converge to the same equilibrium value.

Regeneration Desorption of metals may be carried out under acidic conditions. During the desorption process, metals ions loaded to biomass are replaced by protons diffusing in from the bulk eluant solution. Then, metal ions can diffuse through the permeable biomass towards the particle surface. Finally, the ions diffuse across the stationary liquid layer (film) that surrounds the biomass particles into the bulk solution. The main resistance to the overall desorption process is the internal diffusion (Yang and Volesky 1996). In desorption dynamic experiments film resistance is reduced significantly by stirring. The acid concentration is much higher than the metal concentration in the elution solution and the corresponding increase in pH, which results from proton consumption during desorption, is negligible due to the relatively low amount of metal in the biomass-liquid system. Therefore, no titration is necessary to maintain the pH value. Biosorption and desorption mechanisms are the same, except for the initial boundary conditions and equilibrium relationship. As the regeneration of the biosorbent occurs by ion exchange, the equilibrium is given by the

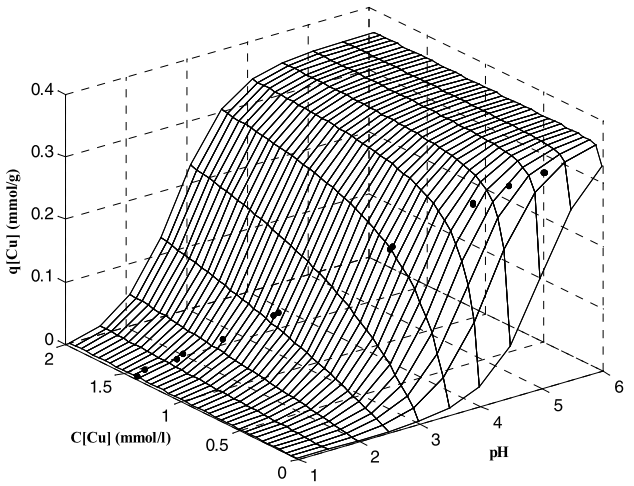

(a)

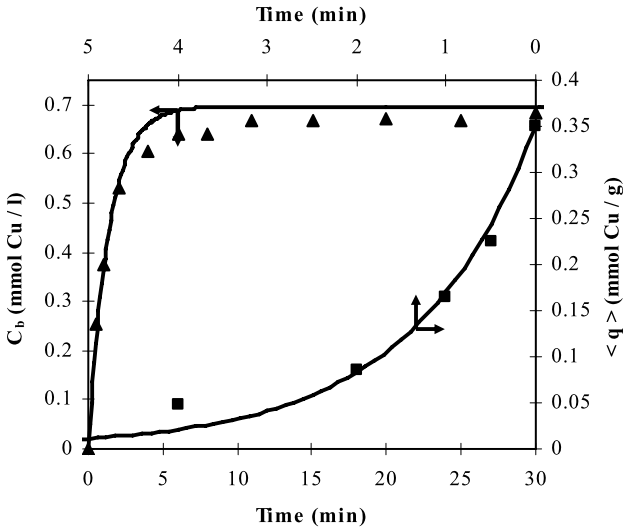

(b)

Fig. 7 **a** Surface representation of the mass action law for algae *Gelidium*; **b** Copper desorption kinetic from loaded algae *Gelidium* with 0.1 M HNO_3

mass action law with 1:1 stoichiometry (Vilar et al. 2007a) (Fig. 7a):

$$q_M = \frac{K_H^M Q_{\max} C_M}{C_T + (K_H^M - 1)C_M}. \tag{14}$$

The acid concentration remains constant and is much higher than metal concentration. As the initial metal loaded is low, the total concentration in the liquid phase is constant and approximately equal to the acid concentration ($C_T = C_M + C_H \approx C_H$). We also can consider that the acid concentration is much higher than the product ($K_H^M C_M$), so the denominator of (14) simplifies to C_H and the equilibrium relationship is reduced to a linear isotherm:

$$q_M = \frac{K_H^M Q_{\max}}{C_H} C_b. \tag{15}$$

This assumption is not valid for desorption in column, because higher biosorbent quantities are used and higher metal loaded concentrations are found.

Integrating the mass balance equation (11) with the limits $t = 0 \rightarrow \langle q \rangle = q_{M_0}$; $C_b = C_{M_0} = 0$ and $t = t \rightarrow \langle q \rangle = \langle q \rangle$; $C_b = C_b$, we will get:

$$\langle q \rangle = q_{M_0} - \frac{V}{W} C_b \tag{16}$$

where q_{M_0} is the amount of metal loaded in the biosorbent (mmol g^{-1}). The initial metal concentration in the liquid phase in a batch system is null, because we only have the eluant solution. As no film resistance is considered, the bulk solution is in equilibrium with the metal loaded in the biosorbent, described by the mass action law.

If we consider the average metal concentration inside the thin plate particles (10), we will get the following ordinary differential equation:

$$\frac{dC_b}{dt} + \frac{W}{V} k_p a_p \left[\left(\frac{K_H^M Q_{\max}}{C_H} + \frac{V}{W} \right) C_b - q_{M_0} \right] = 0. \tag{17}$$

Solving this equation with the initial condition ($t = 0 \rightarrow C_b = C_{M_0} = 0$), the metal concentration in the liquid phase is obtained as a function of time:

$$C_b = \frac{q_{M_0}}{\left(\frac{K_H^M Q_{\max}}{C_H} + \frac{V}{W}\right)} \times \left\{ 1 - \exp\left[-\left(1 + \frac{W}{V} \frac{K_H^M Q_{\max}}{C_H} \right) k_p a_p t \right] \right\}. \tag{18}$$

The model fits well the experimental data for Cu(II) desorption from algae *Gelidium* as shown in Fig. 7b. The homogeneous diffusion coefficient obtained was 1.0×10^{-7} cm^2 s^{-1}.

3.3.2 Mass transfer model for continuous flow stirred tanks

In a Continuous Stirred Tank Adsorber (CSTA) the outflow composition represents exactly what is inside. This type of contact system allows handling suspensions, makes possible the combination of flow schemes and doesn't need immobilization of the biomass to maintain the integrity of the adsorbent particles, if there is a biosorbent filtration step. Different studies have been performed in CSTR coupled with microfiltration and/or ultrafiltration systems, for biomass recovery (Barba et al. 2001; Beolchini et al. 2001, 2004, 2005; Reddad et al. 2003; Pagnanelli et al. 2004). In this study, the

biosorbent was packed in hampers to avoid biomass loss and attrition.

In order to predict the concentration profile inside the CSTA for the saturation and regeneration steps, two mass transfer models are presented below.

Saturation A model was developed with the following assumptions: isothermal operation, adsorption equilibrium described by the Langmuir isotherm, external (film) resistance to mass transfer, and internal mass transfer resistance described by the LDF approximation. The model equations are:

Mass conservation in the fluid around particles

$$\frac{dy'_b(\theta)}{d\theta} = 1 - y'_b(\theta) - \xi' \frac{d\langle y'(\theta)\rangle}{d\theta}. \tag{19}$$

Mass conservation inside particles (LDF-Linear Driving Force)

$$\frac{d\langle y'(\theta)\rangle}{d\theta} = N_d(y^*(\theta) - \langle y'(\theta)\rangle). \tag{20}$$

Assuming that there is no accumulation in the fluid film surrounding particles, we can write:

$$\frac{d\langle y'(\theta)\rangle}{d\theta} = \frac{N_f}{\xi'}(y'_b(\theta) - y'_f(\theta)). \tag{21}$$

Equaling (20) to (21) we will get:

$$\frac{N_f}{\xi'}(y'_b(\theta) - y'_f(\theta)) = N_d[y^*(\theta) - \langle y'(\theta)\rangle]. \tag{22}$$

Initial conditions can be set as,

$$\begin{aligned} &\theta = 0, \qquad y'_b(\theta) = 0, \\ &y'_f(\theta) = 0, \qquad \langle y'(\theta)\rangle = 0. \end{aligned} \tag{23}$$

The dimensionless variables are:

$$y'_b(\theta) = \frac{C_b(t)}{C_E}, \qquad y'_f(\theta) = \frac{C_f(t)}{C_E},$$

$$\langle y'(\theta)\rangle = \frac{\langle q(t)\rangle}{q_E}, \qquad y^*(\theta) = \frac{q_M(t)}{q_E}$$

and the dimensionless parameters are:

$$\tau = \frac{\varepsilon V_r}{Q}, \qquad \tau_d = \frac{R^2}{D_h}, \qquad \tau_d^* = \frac{1}{k_p a_p} = \frac{\tau_d}{3},$$

$$\tau_f = \frac{\varepsilon}{(1-\varepsilon)}\frac{1}{k_f a_p}, \qquad \xi' = \frac{(1-\varepsilon)}{\varepsilon}\rho_{ap}\frac{q_E}{C_E},$$

$$N_f = \frac{\tau}{\tau_f} = \frac{(1-\varepsilon)}{\varepsilon}k_f a_p \tau, \qquad N_d = \frac{\tau}{\tau_d^*} = k_p a_p \tau$$

where $q_E = Q_{\max} K_L C_E/[1 + K_L C_E]$ is the solid phase concentration in equilibrium with C_E.

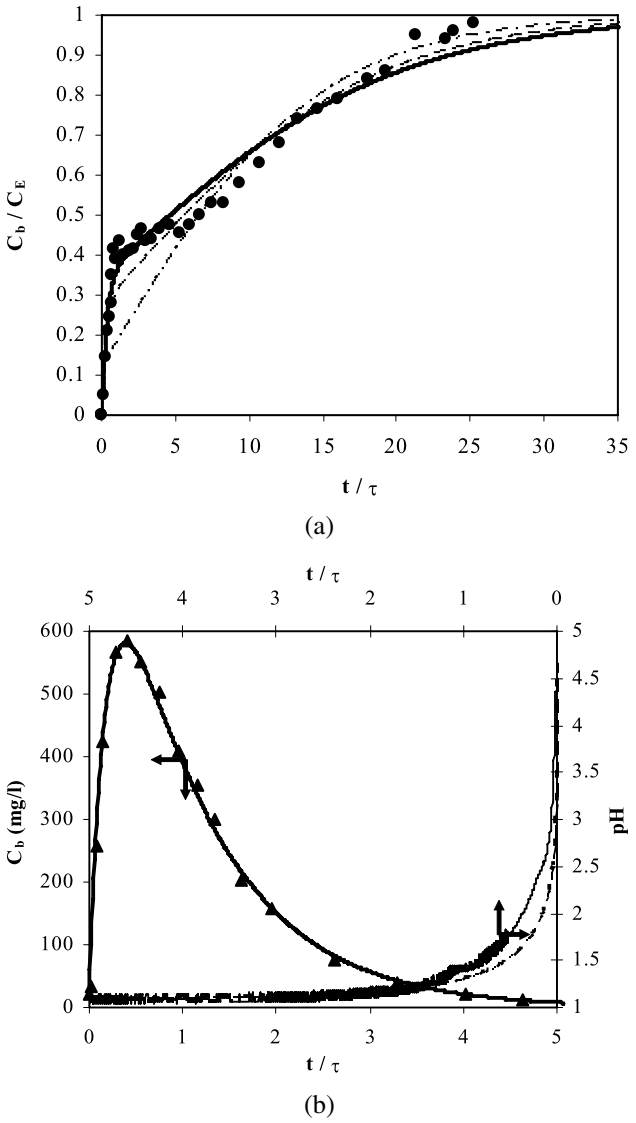

Fig. 8 Experimental data and simulated concentration profiles for Cu(II) continuous biosorption at 100 rpm **(a)** and Pb(II) elution at 243 rpm **(b)** onto algae *Gelidium* in a CSTA

The system of (19) and (20) in conjunction with the initial conditions (23), was solved by LSODA subroutine (Hindmarsh 1983), where y'_f is obtained by solving (22) and the equilibrium is given by the Langmuir isotherm.

The biosorption results of Cu(II) by algae *Gelidium* in a CSTA are showed in Fig. 8a using a Cu(II) concentration of 25 mg l^{-1}. The film mass transfer coefficient, k_f, can be obtained from the "knee" of the breakthrough curve (Rodrigues and Beira 1979). Simulated curves for three different values of k_f (Fig. 8a) confirm that decreasing k_f (increasing the film resistance) the "knee" height increases.

Regeneration An elution model was developed with the following assumptions: isothermal operation, adsorption equilibrium described by the mass action law and internal

mass transfer resistance described by the LDF approximation. All concentrations are expressed in mmol l^{-1}.

Mass conservation in the fluid around particles

$$\frac{dy'_b}{d\theta} = -y'_b - \xi'' \frac{d\langle y\rangle}{d\theta}. \tag{24}$$

Total mass conservation in the fluid around particles

$$\frac{dy_T}{d\theta} = \frac{C_{T_E}}{C_{T_0}} - y_T \tag{25}$$

where the new dimensionless variables are defined as:

$$y_T = \frac{C_T}{C_{T_0}}, \qquad y'_b = \frac{C_b}{C_{T_0}},$$
$$C_T = C_b + C'_b, \qquad C_{T_0} = C_{b_0} + C'_{b_0}.$$

The dimensionless parameters are the same considered before, with the exception of the column capacity factor, which is now defined as:

$$\xi'' = \frac{(1-\varepsilon)}{\varepsilon}\rho_{ap}\frac{Q_{\max}}{C_{T_0}}.$$

Applying the dimensionless variables to (14), we get:

$$y^* = \frac{K_H^M y'_b}{y_T + (K_H^M - 1)y'_b}. \tag{26}$$

Initial conditions:

$$\theta = 0, \qquad y'_b = \frac{C_{b_0}}{C_{T_0}}, \qquad y_T = 1, \qquad \langle y\rangle = \frac{q_{M0}}{Q_{\max}}. \tag{27}$$

Resolution of (20), (24) and (25) in conjunction with the initial conditions (27), were solved by LSODA subroutine (Hindmarsh 1983), where equilibrium is given by the mass action law (26).

The simulated curves fit well to the experimental Cu(II) and pH profiles (Fig. 8b), and confirm that, in this system, elution is an ion exchange process.

3.3.3 *Mass transfer models for continuous flow columns*

For process design and optimization two mass transfer models for the saturation and regeneration steps in a continuous-flow fixed bed sorption column were developed.

Saturation The saturation model was developed with the following assumptions: isothermal operation, axial dispersed plug flow of the fluid phase, adsorption equilibrium described by the Langmuir isotherm, external (film) resistance to mass transfer, and internal mass transfer resistance described by the LDF approximation.

Mass conservation in the fluid around particles:

$$\frac{\partial y'_b(x,\theta)}{\partial\theta} = \frac{1}{Pe}\frac{\partial^2 y'_b(x,\theta)}{\partial x^2} - \frac{\partial y'_b(x,\theta)}{\partial x} - \xi' N_d[y^*(x,\theta) - \langle y'(x,\theta)\rangle] \tag{28}$$

with the initial and boundary conditions:

$$\theta = 0: \quad y'_b(x,0) = y'_f(x,0) = \langle y'(x,0)\rangle = 0, \tag{29}$$

$$x = 0: \quad -\frac{1}{Pe}\frac{\partial y'_b(x,\theta)}{\partial x} + y'_b(x,\theta) = 1, \tag{30}$$

$$x = 1: \quad \left.\frac{\partial y'_b(x,\theta)}{\partial x}\right|_{x=1} = 0. \tag{31}$$

The new dimensionless variables are defined as:

$$x = \frac{z'}{L}, \qquad \langle y'(x,\theta)\rangle = \frac{\langle q(z',t)\rangle}{q_E},$$
$$y^*(x,\theta) = \frac{q_M(z',t)}{q_E}. \tag{32}$$

And the new dimensionless parameters as:

$$\tau = \frac{L}{u_i}, \qquad Pe = \frac{u_i L}{D_{ax}}. \tag{33}$$

The partial differential (28) in conjunction with the initial and boundary conditions, (29), (30) and (31), were solved by the PDECOL package (Madsen and Sincovec 1979), where $y'_f(x,\theta)$ is obtained by solving (22) and the equilibrium is given by the Langmuir isotherm.

Figure 9a shows that the mass transfer models describe well the experimental results at different initial feed pH solutions. For higher values of the influent pH, the breakthrough time increases (Fig. 9a), since the metal uptake capacity at the equilibrium also increases.

Equilibrium parameters were obtained considering the final pH of the breakthrough curve, which is the equilibrium pH inside the column. Biosorption of metal ions by algae *Gelidium* is accomplished by the release of H^+, K^+, Na^+, Ca^{2+}, Mg^{2+} and other ions, due to ion exchange mechanism. Since the metal ions can bind to surface groups by exchange with ions other than H^+, most of them not affecting the solution pH, it was not possible to model the pH profile. The axial Peclet number based on the particle diameter, $Pe_p = u_i d_p / D_{ax}$, is normally around 2 (Froment and Bischof 1990); this value was used to calculate $Pe = 2L/d_p$, which is very high, suggesting that axial dispersion is negligible, but it was included in the model.

Regeneration The regeneration model was developed with the following assumptions: isothermal operation, axial dispersed plug flow of the fluid phase, adsorption equilibrium described by the mass action law, external (film) resistance

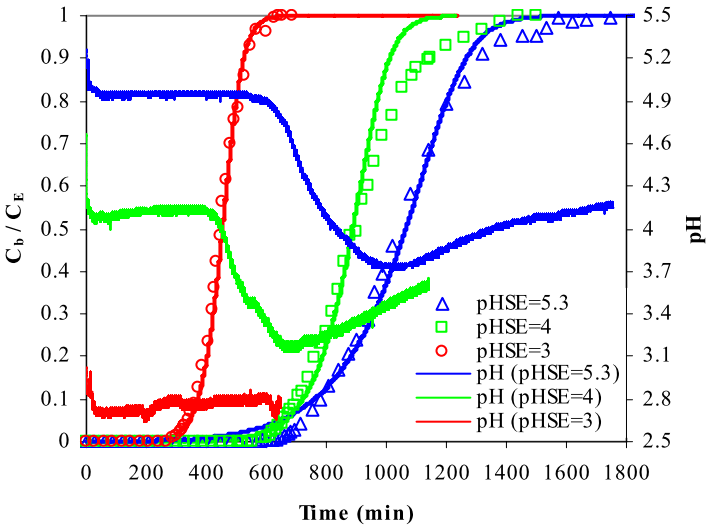

(a)

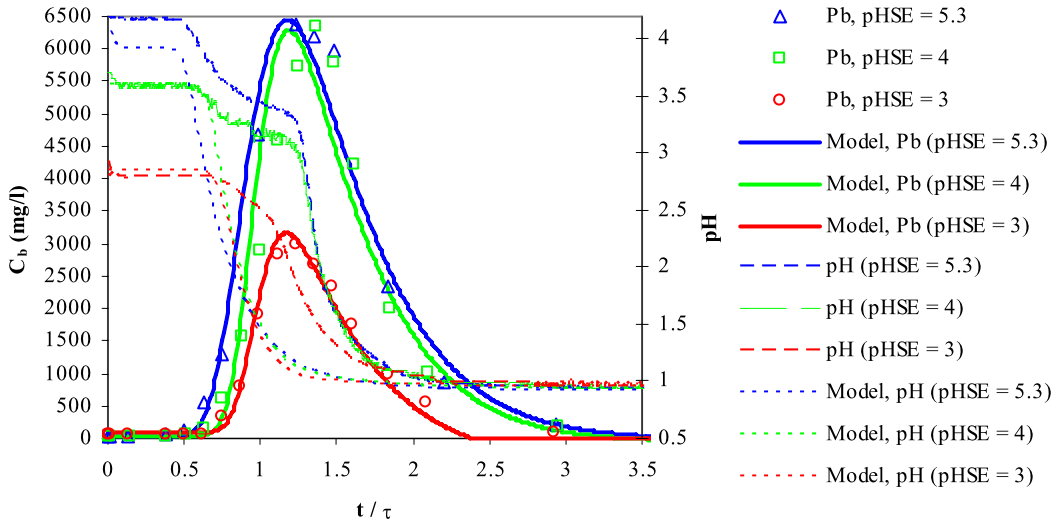

(b)

Fig. 9 Experimental data and simulated concentration profiles for continuous Pb(II) biosorption **(a)** and elution **(b)** onto algae *Gelidium* in a packed bed column at different feed solution pH

to mass transfer, and internal mass transfer resistance described by the LDF approximation.

Mass conservation in the fluid around particles

$$\frac{\partial y_T(x,\theta)}{\partial \theta} = \frac{1}{Pe}\frac{\partial^2 y_T(x,\theta)}{\partial x^2} - \frac{\partial y_T(x,\theta)}{\partial x}. \tag{34}$$

The new dimensionless variables are:

$$y'_b(x,\theta) = \frac{C_b(z',t)}{C_{T_0}}, \qquad y'_f(x,\theta) = \frac{C_f(z',t)}{C_{T_0}},$$
$$y'_T(x,\theta) = \frac{C_T(z',t)}{C_{T_0}}, \qquad \langle y'(x,\theta)\rangle = \frac{\langle q(z',t)\rangle}{Q_{\max}}, \tag{35}$$
$$y^*(x,\theta) = \frac{q_M(z',t)}{Q_{\max}}.$$

The initial and boundary conditions are:

$$\theta = 0: \quad y'_b(x,0) = \frac{C_{b_0}}{C_{T_0}}, \qquad y'_f(x,0) = \frac{C_{b_0}}{C_{T_0}},$$
$$y_T(x,0) = 1, \qquad \langle y'(x,0)\rangle = \frac{q_{M_0}}{Q_{\max}}, \tag{36}$$

$$x = 0: \quad -\frac{1}{Pe}\frac{\partial y'_b(x,\theta)}{\partial x} + y'_b(x,\theta) = 0, \tag{37}$$

$$-\frac{1}{Pe}\frac{\partial y_T(x,\theta)}{\partial x} + y_T(x,\theta) = \frac{C_{T_E}}{C_{T_0}}, \tag{38}$$

$$x = 1: \quad \left.\frac{\partial y'_b(x,\theta)}{\partial x}\right|_{x=1} = \left.\frac{\partial y_T(x,\theta)}{\partial x}\right|_{x=1} = 0 \tag{39}$$

where C_{T_E} is equal to the molar concentration of feed solution (0.1 M HNO_3) and C_{T_0} is the sum of the metal and proton concentrations in the interstitial fluid inside the column at the end of the saturation process.

The partial differential equation (28) and (34) in conjunction with the initial and boundary conditions, (36), (37), (38) and (39), were solved by the PDECOL package (Madsen and Sincovec 1979), where $y'_f(x,\theta)$ is obtained by solving (22) and the equilibrium is given by the mass action law (26).

Considering the effectiveness of lead desorption from loaded biomass, we concluded that desorption was 100% effective and rapid, even for high values of the solid to liquid ratio, leading to high values of the concentration factor (Fig. 9b). The difference between experimental and predicted pH profile (Fig. 9b) can be due to the fact that in the elution model it was assumed that after biomass saturation the binding sites were only occupied by metal ions and protons. However, some binding groups are occupied by other ions as Na^+, K^+, Mg^{2+}, Ca^{2+} and a greater consumption of H^+ is required to replace these ions. As this consumption was not taken into account, the pH profile predicted by the model shows a higher decrease compared with the experimental one.

4 Conclusions

The characterization of the biosorbents before biosorption studies, in order to determine the main characteristics of the biosorbent, principally the binding groups responsible by the metal uptake, is essential. The biosorbents can be considered as a heterogeneous biomass, following a Quasi-Gaussian affinity constant distribution. The NICA model, considering a continuous distribution of the binding sites, can be used to describe the equilibrium metal uptake data at different pH. A mass action law, considering desorption as an ion exchange process, was successfully applied to describe desorption of Cu(II) from algae *Gelidium*. A mass transfer model was applied to the biosorption and desorption kinetic data in a batch system in order to obtain the homogeneous diffusion coefficients necessary for application in continuous systems. The continuous biosorption/desorption in a CSTA and packed bed column was well described by a mass transfer model, which can be used for process design of real metal-bearing effluents, and future application in industrial water treatment processes.

Acknowledgements Financial support by FCT and European Community through FEDER (project POCI/AMB/57616/2004) is gratefully acknowledged. The authors are grateful to FCT for V. Vilar's doctorate scholarship (SFRH/BD/7054/2001).

References

Al-Ashed, S., Duvnjak, Z.: Adsorption of copper and chromium by *Aspergillus carbonarius*. Biotechnol. Prog. **11**, 638–642 (1995)

Atkinson, B., Bux, F., Kasan, H.: Considerations for application of biosorption technology to remediate metal-contaminated industrial effluents. Water SA **24**(2), 129–135 (1998)

Babel, S., Kurniawan, T.A.: Low-cost adsorbents for heavy metals uptake from contamined water: a review. J. Hazard. Mater. **B97**, 219–243 (2003)

Bailey, S.E., Olin, T.J., Bricka, R.M., Adrian, D.D.: A review of potentially low-cost sorbents for heavy metals. Water Res. **33**(11), 2469–2479 (1999)

Barba, D., Beolchini, F., Vegliò, F.: A simulation study on biosorption of heavy metals by confined biomass in UF/MF membrane reactors. Hydrometallurgy **59**, 89–99 (2001)

Beolchini, F., Pagnanelli, F., Vegliò, F.: Modeling of copper biosorption by *Arthrobacter sp*. in a UF/MF membrane reactor. Environ. Sci. Technol. **35**, 3048–3054 (2001)

Beolchini, F., Pagnanelli, F., Toro, L., Vegliò, F.: Copper biosorption by *Sphaerotilus natans* confined in UF membrane module: experimental study and kinetic modeling. Hydrometallurgy **72**, 21–30 (2004)

Beolchini, F., Pagnanelli, F., Toro, L., Vegliò, F.: Continuous biosorption of copper and lead in single and binary systems using *Sphaerotilus natans* cells confined by a membrane: experimental validation of dynamic models. Hydrometallurgy **76**, 73–85 (2005)

Brunauer, S., Emmett, P.H., Teller, E.: Adsorption of gases in multimolecular layers. J. Am. Chem. Soc. **60**, 309–319 (1938)

Davis, T.A., Volesky, B., Mucci, A.: A review of the biochemistry of heavy metal biosorption by brown algae. Water Res. **37**, 4311–4330 (2003)

Dean, J.A.: Lange's Handbook of Chemistry, 12th edn. McGraw–Hill, New York (1979)

Freundlich, H.: Üeber die Adsorption in Löesungen. Z. Phys. Chem. **57**, 385–470 (1907)

Froment, G.F., Bischof, K.B.: Chemical Reactor Analysis and Design. Wiley, New York (1990)

Gavrilescu, M.: Removal of heavy metals from the environment by biosorption. Eng. Life Sci. **4**(3), 219–231 (2004)

Glueckauf, E., Coates, J.I.: Theory of chromatography. Part IV. The influence of incomplete equilibrium on the front boundary of chromatograms and on the effectiveness of separation, J. Chem. Soc. pp. 1315–1321 (1947)

Hindmarsh, A.C.: Odepack, a Systematized Collection of ODE Solvers, in Scientific Computing. Scientific Computing, Amsterdam (1983)

Kinniburgh, D.G., Riemsdijk, W.H.V., Koopal, L.K., Borkovec, M., Benedetti, M.F., Avena, M.J.: Ion binding to natural organic matter: competition, heterogeneity, stoichiometry and thermodynamic consistency. Colloids Surf. A **151**, 147–166 (1999)

Kratochvil, D., Volesky, B.: Biosorption of Cu from ferruginous wastewater by algal biomass. Water Res. **32**(9), 2760–2768 (1998)

Langmuir, I.: The adsorption of gases on plane surfaces of glass, mica and platinum. J. Am. Chem. Soc. **40**, 1361–1403 (1918)

Madsen, N., Sincovec, R.: PDECOL: General collocation software for partial differential equations. ACM Trans. Math. Soft. **5**(3), 326–351 (1979)

Matheickal, J.T., Yu, Q.: Biosorption of lead(II) and copper(II) from aqueous solutions by pre-treated biomass of Australian marine algae. Biores. Technol. **69**(3), 223–229 (1999)

Mouradi-Givernaud, A., Hassani, L.A., Givernaud, T., Lemoine, Y., Benharbet, O.: Biology and agar composition of *Gelidium sesquipedale* harvested along the Atlantic coast of Morocco. In: Hydrobiologia, pp. 391–395 (1999)

Nieboer, E., McBryde, W.A.E.: Free-energy relationship in coordination chemistry, III: a comprehensive index to complex stability. Can. J. Chem. **51**, 2512–2524 (1973)

Pagnanelli, F., Beolchini, F., Biase, A.D., Vegliò, F.: Biosorption of binary heavy metal systems onto *Sphaerotilus natans* cells confined in an UF/MF membrane reactor: dynamic simulations by different Langmuir-type competitive models. Water Res. **38**, 1055–1061 (2004)

Pearson, R.G.: Hard and soft acids and bases. J. Am. Chem. Soc. **85**, 3533–3539 (1963)

Radke, C.J., Prausnitz, J.M.: Adsorption of organic solutes from dilute aqueous solution of activated carbon. Ind. Eng. Chem. Fundam. **11**(4), 445–451 (1972)

Reddad, Z., Gérente, C., Andrès, Y., Thibault, J.-F., Cloirec, P.L.: Cadmium and lead adsorption by a natural polysaccharide in Mf membrane reactor: experimental analysis and modeling. Water Res. **37**, 3983–3991 (2003)

Redlich, O., Peterson, C.: Useful adsorption isotherm. J. Phys. Chem. **63**, 1024 (1959)

Reid, R.C., Prausnitz, J.M., Poling, B.E.: The Properties of Gases & Liquids, 4th edn. McGraw–Hill, New York (1987)

Rodrigues, A.E., Beira, E.C.: Staged approach to percolation processes. Part I. Sorption processes in a perfectly mixed reactor: influence of nonlinear equilibrium isotherm and external mass transfer resistance, AIChE J. **25**, 416–423 (1979)

Sips, R.: On the structure of a catalyst surface. J. Chem. Phys. **16**, 490–495 (1948)

Vignon, M.R., Morgan, E., Rochas, C.: *Gelidium sesquipedale* (*Gelidiales*, *Rhodophyta*), I: soluble polymers. Bot. Mar. **37**, 325–329 (1994a)

Vignon, M.R., Rochas, C., Vuong, R., Tekeley, P., Chanzy, H.: *Gelidium sesquipedale* (*Gelidiales*, *Rhodophyta*), II: an untrastructural and morphological study. Bot. Mar. **37**, 331–340 (1994b)

Vilar, V.J.P.: Remoção de iões metálicos em solução aquosa por resíduos da indústria de extracção do agar. PhD thesis, Faculty of Engineering University of Porto, Porto (2006)

Vilar, V.J.P., Botelho, C.M.S., Boaventura, R.A.R.: Influence of pH, ionic strength and temperature on lead biosorption by *Gelidium* and agar extraction algal waste. Proc. Biochem. **40**(10), 3267–3275 (2005a)

Vilar, V.J.P., Sebesta, F., Botelho, C.M.S., Boaventura, R.A.R.: Equilibrium and kinetic modeling of Pb^{2+} biosorption by granulated agar extraction algal waste. Proc. Biochem. **40**(10), 3276–3284 (2005b)

Vilar, V.J.P., Botelho, C.M.S., Boaventura, R.A.R.: Equilibrium and kinetic modeling of Cd(II) biosorption by algae *Gelidium* and agar extraction algal waste. Water Res. **40**(2), 291–302 (2006a)

Vilar, V.J.P., Botelho, C.M.S., Boaventura, R.A.R.: Methylene blue adsorption by algal biomass based materials: biosorbents characterization and process behavior. J. Hazard. Mater., doi:10.1016/j.jhazmat.2006.1012.1055 (2006b)

Vilar, V.J.P., Botelho, C.M.S., Boaventura, R.A.R.: Copper desorption from *Gelidium* algal biomass. Water Res. **41**(7), 1569–1579 (2007a)

Vilar, V.J.P., Botelho, C.M.S., Boaventura, R.A.R.: Copper removal by algae *Gelidium*, agar extraction algal waste and granulated algal waste: kinetics and equilibrium. Biores. Technol., doi:10.1016/j.biortech.2007.01.042 (2007b)

Vilar, V.J.P., Botelho, C.M.S., Boaventura, R.A.R.: Kinetics and equilibrium modeling of lead uptake by algae *Gelidium* and algal waste from agar extraction industry. J. Hazard. Mater. **143**(1–2), 396–408 (2007c)

Volesky, B.: Biosorption of Heavy Metals. CRC Press, Montreal (1990)

Volesky, B.: Detoxification of metal-bearing effluents: biosorption for the next century. Hydrometallurgy **59**, 203–216 (2001)

Volesky, B.: Sorption and Biosorption, 1st edn. BV Sorbex, Quebec (2003)

Wase, J., Forster, C.: Biosorbents for Metal Ions. Taylor & Francis, London (1997)

Yang, J., Volesky, B.: Intraparticle diffusivity of Cd ions in a new biosorbent material. J. Chem. Technol. Biotechnol. **66**, 355–364 (1996)